



Contributions of dust and biomass-burning to aerosols at a Colorado mountain-top site

A. G. Hallar et al.

Contributions of dust and biomass-burning to aerosols at a Colorado mountain-top site

A. G. Hallar¹, R. Petersen¹, E. Andrews^{2,3}, J. Michalsky^{2,3}, I. B. McCubbin¹, and J. A. Ogren²

¹Storm Peak Laboratory, Desert Research Institute, Steamboat Springs, CO, USA

²NOAA Earth System Research Laboratory, Boulder, USA

³Cooperative Institute for Research in Environmental Sciences, University of Colorado, Boulder, CO, USA

Received: 10 July 2015 – Accepted: 21 July 2015 – Published: 7 August 2015

Correspondence to: A. G. Hallar (ghallar@dri.edu)

Published by Copernicus Publications on behalf of the European Geosciences Union.

Title Page

Abstract

Introduction

Conclusions

References

Tables

Figures



Back

Close

Full Screen / Esc

Printer-friendly Version

Interactive Discussion



Abstract

Visible Multifilter Rotating Shadowband Radiometer (MFRSR) data were collected at Storm Peak Laboratory (SPL), a mountain top facility in northwest Colorado, from 1999–2011 and in 2013. From 2011–2014, in situ measurements of aerosol light scattering were also obtained. Using these datasets together, the seasonal impact of dust and biomass burning is considered for the western United States. Analysis indicates that the median contributions to spring and summer aerosol optical depth (AOD) from dust and biomass-burning aerosols across the dataset are comparable. The mean AOD is slightly greater in the summer, with significantly more frequent and short duration high AOD measurements due to biomass-burning episodes, than in the spring. The Ångström exponent showed a significant increase in the summer for both the in situ and MFRSR data, indicating an increase in combustion aerosols. Spring dust events are less distinguishable in the in situ data than the column measurement, suggesting that a significant amount of dust may be found above the elevation of SPL, 3220 m a.s.l.

Twenty-two known case studies of intercontinental dust, regional dust, and biomass burning events were investigated. These events were found to follow a similar pattern, in both aerosol loading and Ångström exponent, as the seasonal mean signal in both the MFRSR and ground-based nephelometer. This dataset highlights the wide scale implications of a warmer, drier climate on visibility in the western United States.

1 Introduction

The effect of aerosol particles is critical in understanding Earth's radiation budget, yet significant uncertainties in the radiative properties of aerosols globally and on regional scales prevent the needed accuracy within numerical models to define future climate change. When considering only the direct effect of aerosols on global climate, the Intergovernmental Panel on Climate Change (IPCC) uncertainty estimate is currently greater than the effect at $-0.35 \pm 0.5 \text{ W m}^{-2}$ and in urgent need of further research

Contributions of dust and biomass-burning to aerosols at a Colorado mountain-top site

A. G. Hallar et al.

Title Page

Abstract

Introduction

Conclusions

References

Tables

Figures



Back

Close

Full Screen / Esc

Printer-friendly Version

Interactive Discussion



Contributions of dust and biomass-burning to aerosols at a Colorado mountain-top site

A. G. Hallar et al.

Title Page

Abstract

Introduction

Conclusions

References

Tables

Figures

◀

▶

◀

▶

Back

Close

Full Screen / Esc

Printer-friendly Version

Interactive Discussion

(Boucher et al., 2013). As the radiative impact depends on aerosol composition and size, characterization of the aerosol population is necessary. Furthermore, understanding the source region of the aerosol is critical for emission control policy both for air quality and visibility. In 1977, the Clean Air Act amendments began regulating visibility in 156 Class I areas, which include many national wilderness areas and memorial parks (Watson, 2002). A majority of these areas are in the western United States most recently, The U.S. Environmental Protection Agency (EPA) Regional Haze Rule (U.S. EPA, 2003) mandated a schedule of increasing emission controls to achieve “natural visibility conditions” in these Class I areas by 2064. Unlike the rest of the United States, visibility has not improved in the intermountain/southwest (–116 to –100° longitude) regions over the last two decades (Hand et al., 2014) and, in fact, some aerosol contributors to visibility degradation are increasing.

Tangible evidence for intercontinental transport of pollution associated with desert dust and smoke from biomass burning has changed air pollution from a local issue to one of global scope (Akimoto, 2003). Remote locations in the western United States are influenced both by domestic emissions and intercontinental transport of aerosols (e.g., Bodhaine, 1996; Yu et al., 2012). For example, an analysis by VanCuren and Cahill (2002) of the long-term data set provided by the Interagency Monitoring for Protected Visual Environments (IMPROVE) network indicated that Asian outflow including mineral dust is a frequent component of the lower free troposphere over much of North America, implying that Asian outflow to the United States is not solely limited to episodic spring-time episodes. In a later study with three sites in California located at different elevations, VanCuren et al. (2005) demonstrated a distinct separation between the stable marine boundary layer and the troposphere. This layer separation resulted in isolation of free tropospheric air, allowing mountain sites (> 2 km) to be consistently dominated by Asian continental aerosols. Kavouras et al. (2009) identified 610 days between 2001 and 2003 where dust was the major contributor to severe visibility reduction in an area of the western United States. Using a variety of techniques, they assigned dust origins to local, regional, or trans-boundary (Asian) sources on 496 of

Contributions of dust and biomass-burning to aerosols at a Colorado mountain-top site

A. G. Hallar et al.

[Title Page](#)[Abstract](#)[Introduction](#)[Conclusions](#)[References](#)[Tables](#)[Figures](#)[◀](#)[▶](#)[◀](#)[▶](#)[Back](#)[Close](#)[Full Screen / Esc](#)[Printer-friendly Version](#)[Interactive Discussion](#)

those days. In contrast to previous studies, dust sources were predominantly local (201 cases) and regional (240 cases). Asian sources were most significant on only 55 days, mainly during spring. Fischer et al. (2009) combined SeaWiFS aerosol optical thickness (AOT) over the Taklamakan and Gobi Deserts with IMPROVE observations in the northwest United States to study surface aerosol variability with regard to Asian dust emissions. Results indicated that a significant (50 %) amount of the interannual variability in springtime average $PM_{2.5}$ and PM_{10} (particles smaller than 2.5 and 10 μm in diameter, respectively) can be explained by Asian dust emissions. Overall, as shown by Yu et al. (2008), spring is the most active season for trans-Pacific transport of aerosols due to the active extratropical cyclones combined with strong mid-latitude westerlies, however, this transport occurs throughout the year. More recently, by integrating satellite measurements, Yu et al. (2012) found that interannual variations of AOD over the North Pacific basin are smaller for dust than combustion aerosols and likely attributable to Eurasian fires (i.e. especially large fires in 2003 and 2008). Consistent with the prior studies, the trans-Pacific dust dominates the imported aerosol mass (88 %) relative to combustion aerosol (6 %), and transport occurs predominately above the boundary layer, resulting in elevated dust layers at 2–6 km (Yu et al., 2012). Previously Asian dust was observed at Storm Peak Laboratory, a mountain-top laboratory in Northern Colorado, associated with a high pressure system and elevated levels of gaseous elemental mercury (Obrist et al., 2008).

Human activities such as livestock grazing have also increased dust in the western interior United States by disturbing natural, stable surfaces such as cryptobiotic soils and physical crusts in the extensive deserts (Belnap and Gillette, 1998; Reynolds et al., 2001). With sediment cores from two alpine lakes in the San Juan Mountains of southwest Colorado, Neff et al. (2008) showed that dust accumulation rates over the last 150 years are more than five times greater than the average accumulation over the previous 5000 years. Based on ensemble backtrajectories, geostationary remote sensing data, and the size of the dust particles extracted from snow (i.e., greater than 10 μm), the dust in these sediment cores appears to be predominantly from the west-

Contributions of dust and biomass-burning to aerosols at a Colorado mountain-top site

A. G. Hallar et al.

Title Page

Abstract

Introduction

Conclusions

References

Tables

Figures

◀

▶

◀

▶

Back

Close

Full Screen / Esc

Printer-friendly Version

Interactive Discussion



ern United States. The Upper Colorado River basin currently experiences four to twelve late winter- and spring-time dust deposition events each year (Neff et al., 2008; Painter et al., 2010). Using in situ data from Storm Peak Laboratory and ensemble backtrajectories, Hallar et al. (2011a) presented evidence of aerosol incursions at the mountain site from multiple dust storms originating in the Four Corners region of the western United States during the spring of 2010.

Wildfires are also increasing in the western United States, as shown by a six-fold increase in annual area burned from 1986–2003 in comparison to 1970–1986 (West-erling et al., 2006). Using data from 1984–2011, Dennison et al. (2014) demonstrated significant, increasing trends in the number of large fires and/or total large fire area per year, coinciding with trends of increasing drought severity across the western United States. Augustine et al. (2008) observed increasing AOD in the Intermountain West (Fort Peck, Mt and Table Mountain, CO) from 1997–2007, and attributed this increase to an upsurge in wildfire activity. It is predicted that wildfires will increase summer time organic aerosol concentration by 40 % by the 2050s in the western United States (Spracklen et al., 2009).

Here, we systematically analyze the relative contributions of dust and biomass burning aerosols from intercontinental, local and regional sources (e.g., the Colorado Plateau) with observed aerosol loading at a high altitude site. The analysis was performed using a long-term record of radiometer data (1999–2011 and 2013) coupled with a more recent record (2011–2014) of in situ aerosol optical properties located at a remote mountaintop location in the Rocky Mountains within the western United States.

vis-MFRSR voltage response at the top of the atmosphere. In the absence of clouds, the direct solar irradiance measured by the vis-MFRSR is determined by:

$$V(\lambda) = V_o(\lambda) \exp[-\tau(\lambda)m], \quad (1)$$

where $V(\lambda)$ is the voltage induced by direct solar irradiance at a wavelength λ measured by the vis-MFRSR, and $V_o(\lambda)$ is the equivalent voltage due to direct normal irradiance at the top of the atmosphere as a function of λ . τ is the total column optical depth due to scattering and absorption; and m is the air mass traversed by the direct solar beam relative to the air mass in the zenith direction.

Following methods presented in Michalsky et al. (2001 and 2010) the calibration of the vis-MFRSR wavelength channels is achieved using Langley plots. A Langley plot is a graph of the natural log of the direct solar irradiance vs. air mass within a narrow spectral interval. Langley plots for air masses between 2 and 6, corresponding to measurements made between 60 and 80° from the zenith, were screened for stable conditions and included morning and afternoon periods. The nearest 20 successful Langley results to any day in the MFRSR data stream were then used to provide a calibrated voltage response at the top of the atmosphere (V_o) for the MFRSR wavelength channels for that date. These 20 V_o 's at 500 nm are divided to the corresponding V_o 's at 870 nm, and mean of the V_o 's in the interquartile range of these ratios (Michalsky et al., 2010) is used as the best estimate of the V_o 's for all wavelengths. This procedure eliminates false Langleys in atmospheric conditions that could skew the estimation of V_o (Kiedron and Michalsky, submitted to AMT). A final smoothing fit is applied to the stream of robust V_o values for the times series using a lowess filter, as described in Michalsky et al. (2010). Figure 1 illustrates the results of the calibration using Langley plots. The lowess estimate is used in the final analysis of aerosol optical depth to address the long-term variation in the measured V_o due to the degradation and temperature sensitivity of the MFRSR sensor and to extrapolate to the value of V_o for the beginning and end of a deployment of the MFRSR. The V_o 's are normalized to unit

Contributions of dust and biomass-burning to aerosols at a Colorado mountain-top site

A. G. Hallar et al.

Title Page

Abstract

Introduction

Conclusions

References

Tables

Figures



Back

Close

Full Screen / Esc

Printer-friendly Version

Interactive Discussion



solar distance for the above processing and then adjusted to the earth-sun distance for use on the day when aerosol optical depths are calculated using the calibrated V_o 's.

A comparison between an MFRSR calibrated in this manner and calibration at Mauna Loa Observatory (Michalsky and LeBaron, 2013) has indicated that this technique is robust to within a percent. A calculation of the optical depth using the calibrated value for V_o derived above should be accurate to an optical depth of 0.01. Additional uncertainty could be expected from a changing cosine response of the Lambertian receiver. The cosine response of the Lambertian receiver from the vis-MFRSR instrument at SPL was measured in each of the seven channels in 1998, 2003 and 2012. The measured cosine response was used to reduce data until a new cosine response was measured. For example, the cosine response from 1998 was used until 2003, the 2003 response until 2012, and then the 2012 response for subsequent data reduction. The 1998 and 2003 cosine responses were remarkably similar. There was no final measurement of the cosine response when the detector assembly was rebuilt in 2012. This means that if the cosine response changed during the nine-year period between 2003 and 2012, we do not have a measurement of that change. However, given that the 1998 and 2003 cosine responses were quite similar, we assume that there was little change through 2012. The small change in cosine response between 1998 and 2003 suggests that SPL is a very clean site (little local contamination), which minimizes the Lambertian receiver degradation. The 2012 cosine response would not be expected to resemble the earlier cosine responses because the detector head was completely rebuilt.

2.3.2 Cloud screening of MFRSR data

The primary mechanism used to cloud screen the AOD samples derived from the vis-MFRSR measurements is to examine the short-term stability of the AOD. The cloud screening of AOD data occurs in a two-step process, discarding those measurements whose variability indicates the strong possibility of passing clouds. An AOD measurement is cloud screened if the following conditions are met. In the first step a collection

Contributions of dust and biomass-burning to aerosols at a Colorado mountain-top site

A. G. Hallar et al.

Title Page

Abstract

Introduction

Conclusions

References

Tables

Figures

◀

▶

◀

▶

Back

Close

Full Screen / Esc

Printer-friendly Version

Interactive Discussion



of 8 contiguous data points, the change in optical depth between each AOD measurement cannot exceed 0.02, and the change over the entire collection of measurements cannot exceed more than 0.03 (Michalsky et al., 2010). The second step scales these limits according to the estimated magnitude of the optical depth, e.g., lower limits for low optical depths. In total, 242 000 3 min measurements during 1999–2013 passed the screening methodology, resulting in 2252 daily-averaged, cloud-screened MFRSR data points.

2.3.3 Nephelometer

The nephelometer was calibrated once per year with particle-free air and CO₂. Zero checks on filtered air were performed hourly. The nephelometer data were corrected for truncation and illumination non-idealities, as suggested by Anderson and Ogren (1998). Overall, the uncertainty in scattering arising from nephelometer nonidealities is less than 10 % for submicron particles (e.g., Anderson et al., 1996). For coarse mode particles (diameter greater than 1 micron), the nephelometer uncertainty increases for total scattering (20–50 %). This increase is due to the inability of the nephelometer to sense near-forward scattering, which is an increasingly dominant part of the total scattering for large particles (Anderson et al., 1996). Because we consider all aerosol particles less than 10 micron (not just coarse aerosol) and use hourly-averaged data the uncertainties will tend toward the lower side of the uncertainty range (Sheridan et al., 2002).

2.4 Ångström Exponent

The Ångström exponent (α) is inversely dependent on the mean particle radius. It is a power-law relation of the observed AOD to the particular optical wavelength λ . As a non-dimensional measure of wavelength dependence, α can be calculated from both the MFRSR AOD measurements (τ) and the nephelometer scattering measurements

Contributions of dust and biomass-burning to aerosols at a Colorado mountain-top site

A. G. Hallar et al.

Title Page

Abstract

Introduction

Conclusions

References

Tables

Figures

◀

▶

◀

▶

Back

Close

Full Screen / Esc

Printer-friendly Version

Interactive Discussion



(σ_{sp}):

$$\alpha_{Neph} = \ln(\sigma_{sp,\lambda1}/\sigma_{sp,\lambda2})/\ln(\lambda1/\lambda2) \quad (2a)$$

$$\alpha_{MFRSR} = \ln(\tau_{\lambda1}/\tau_{\lambda2})/\ln(\lambda1/\lambda2) \quad (2b)$$

where $\lambda1$ and $\lambda2$ represent the wavelengths used in the calculation for each instrument:
MFRSR $\lambda1 = 500$ nm, $\lambda2 = 870$ nm; nephelometer $\lambda1 = 450$ nm, $\lambda2 = 700$ nm.

The Ångström exponent varies with size distribution, and thus is frequently employed as a qualitative indicator of aerosol composition. This parameter is well suited to differentiate between smoke and dust-related aerosol populations. Values of α can range from approximately two for submicrometer accumulation mode particles, such as those produced during biomass burning, to near zero for coarse mode aerosols such as dust (e.g., Aryal et al., 2014; Clarke et al., 2007; Russell et al., 2010).

3 Identification of dust and fire events at SPL

In order to investigate seasonal differences in aerosol loading, specific known case studies of dust and biomass burning aerosols reaching SPL were considered. These events were identified from the literature and available datasets, as described below, and highlighted in Table 1.

3.1 Dust events

3.1.1 Intercontinental

Table 1 lists two intercontinental dust events observed at SPL and additional details on this pair of events are provided here. The first dust event resulted from a massive dust storm in Mongolia's Gobi desert in April of 2001, which lofted both mineral dust and biomass burning aerosols. These aerosols were sampled during the Asian Pacific Regional Aerosol Characterization Experiment (ACE-Asia) field studies with aircraft,

Contributions of dust and biomass-burning to aerosols at a Colorado mountain-top site

A. G. Hallar et al.

Title Page

Abstract

Introduction

Conclusions

References

Tables

Figures

◀

▶

◀

▶

Back

Close

Full Screen / Esc

Printer-friendly Version

Interactive Discussion



pyranometers are used in combination. The difference in reflected radiation measured by these paired pyranometers enables the measurement of contaminants such as dust in the snow surface (Painter et al., 2007, 2012; Skiles et al., 2012). These “dust on snow” events are cataloged with wind speed and wind direction, starting in May 2006, and available at: <http://www.codos.org/>. Using this catalog, potential SPL dust events were identified when the wind direction was heading towards SPL (northwest quadrant between 180–270°). Based on HYSPLIT ensemble backtrajectories (Draxler and Rolph, 2015) and the measured wind speed at CSAS, it took approximately 24–48 h for the dust to reach SPL from CSAS. For earlier years (2007–2008), the annual CSAS reports were used to select only the largest dust event each year observed at Senator Beck Basin, and it was estimated that the dust reached SPL in 24 h (Hallar et al., 2011a). From 2009–2010, Aerosol Particle Sizer (APS) data were used to identify the initial start and end time of each event at SPL within the initial window suggested by the CSAS data as described in Hallar et al. (2011a). The mean dust particle size by number during the 2009–2010 dust events was approximately 1 μm . For events between 2011–2013, the nephelometer data were used to identify the initial start and end time of the event at SPL. All regional dust case studies identified in this manner are listed in Table 1.

3.2 Fires

The impact of the wildfires on aerosol loading and air quality over Colorado was analyzed by Val Martin et al. (2013) using AOD measured by the MODerate resolution Imaging Spectroradiometer (MODIS) aboard the Terra satellite in combination with surface $\text{PM}_{2.5}$ (particles smaller than 2.5 μm in diameter) averaged over ten sites within the Colorado Front Range corridor. They classified nine main fire events that were identified between 2000–2012. Via this study these events were investigated further, and those with available data from SPL are listed within Table 1. For example, from 3–7 June 2011, Storm Peak Laboratory was strongly impacted by outflow from the Wallow fire in Arizona. The Wallow fire is Arizona’s largest recorded wildfire to date

Contributions of dust and biomass-burning to aerosols at a Colorado mountain-top site

A. G. Hallar et al.

Title Page

Abstract

Introduction

Conclusions

References

Tables

Figures

◀

▶

◀

▶

Back

Close

Full Screen / Esc

Printer-friendly Version

Interactive Discussion

median spring and summer AOD, over this 13-year record, is small (> 0.01). In contrast to the relatively small difference in AOD in the spring and summer, there is a significant difference in the Ångström exponent between those two seasons. The average Ångström exponent during the spring is 0.912 ± 0.0024 (median = 0.865), while during the peak summer season the Ångström exponent is 1.64 ± 0.01 (median = 1.65). From 1 April to 15 May (DOY 91–136), the Ångström exponent shows a further decrease, with an average value of 0.876 ± 0.0028 (median = 0.832), this period is denoted in Fig. 3 with vertical dashed lines.

This pattern suggests a difference in the aerosol size between the spring and summer observed at Storm Peak Laboratory. Specifically, there is an increase in coarse-mode aerosol loading during the spring, with the strongest signal in April and early May (DOY 91–136) when the lowest Ångström exponent values occur. This finding is consistent with the previous work, denoting springtime transport of dust, both from local and remote sources to this region (e.g. Yu et al., 2012; Hallar et al., 2011). Using nephelometer scattering data from approximately 1000 vertical profiles during numerous aircraft campaigns, Clarke et al. (2010) calculated α_{Neph} from scattering at 450 and 700 nm, and then used $\alpha_{\text{Neph}} > 1.3$ to separate air masses consisting of smaller particles characteristic of combustion sources, from air masses consisting of larger dust particles. At SPL, the summer aerosol appears to be dominated by smaller particles. Given the remote nature of SPL, these smaller aerosol particles are most likely combustion aerosol from biomass burning.

The MFRSR and nephelometer instruments cover different time periods, and the plots (top and bottom panels of Fig. 3) show different (though related) aerosol parameters; therefore they should not be expected to be identical. Nonetheless, they present a somewhat consistent picture of the seasonal cycle of loading and particle size. Similar to the MFRSR, the nephelometer measurements show that there is a strong summer peak in aerosol loading due to biomass burning events. However, the nephelometer does not show the increase in loading in the spring that is seen by MFRSR AOD and attributed to dust.

The nephelometer-derived Ångström exponent is higher in the summer than in other times of year (note: this figure shows only one summer of nephelometer measurements (2012) due both to construction downtime and instrument issues). As with the MFRSR, the lowest nephelometer Ångström exponent values occur in the spring, but the dip in Ångström exponent values derived from the nephelometer occurs about a month earlier in the seasonal cycle (1 March–15 April, DOY 60–105) than is observed for the MFRSR-derived Ångström if exponent.

5 Investigating seasonal patterns in relation to known case studies

Using the case studies outlined above, specific events of dust and biomass burning aerosols observed at SPL will be considered, in relationship to seasonal patterns. A scatter plot showing AOD vs. Ångström exponent is a common tool to classify aerosol types, as it can provide information on aerosol loading and size (type) simultaneously (Toledano et al., 2007). Figure 4 presents the relationship between Ångström exponent and aerosol loading for the vis-MFRSR and nephelometer, respectively. Figure 4 identifies the data by spring and summer season using small colored symbols (green and red, respectively) and highlights events listed in Table 1 using large colored symbols as indicated in the legend.

For both instruments, different relationships exist between aerosol loading and the Ångström exponent, indicating that the aerosol load at SPL contains two distinct aerosol populations. The Ångström exponent increases with increasing AOD during the summer, and the Ångström exponent decreases with increasing AOD during the spring. Thus, the aerosol population contains larger particles, consistent with dust, in the spring and smaller particles are observed in the summer months, which is consistent with biomass burning. This relationship between particle size and source is further established by highlighting the case studies in Table 1 by using larger symbols on Fig. 4.

Contributions of dust and biomass-burning to aerosols at a Colorado mountain-top site

A. G. Hallar et al.

Title Page

Abstract

Introduction

Conclusions

References

Tables

Figures

◀

▶

◀

▶

Back

Close

Full Screen / Esc

Printer-friendly Version

Interactive Discussion

For example, a 2001 dust storm originating in Mongolia (e.g. Seinfeld et al., 2004) was measured at SPL and is denoted in Fig. 4a as “2001 Asian Dust”. At SPL, the dust was measured with several instruments including the aerodynamic particle sizer (APS, TSI, Inc.), with an aerosol mode at 2 μm . The 2001 Asian dust event is notable in that it is well defined in the vis-MFRSR measurements for that year relative to other sources of AOD. During the event, the Ångström exponent decreased to 0.17 at SPL on 15 April, highlighting the large particle size. This finding is consistent with other measurements of this event at western, mid-western and eastern United States sun photometer stations, showing similar low Ångström exponents during this week (Thulasiraman et al., 2002). The 2006 Asian dust event (“2006 Asian Dust” on Fig. 4a) shows a similar relationship between Ångström exponent and AOD as was observed for the 2001 event. Ensemble HYSPLIT backtrajectories (Draxler and Rolph, 2015) indicate that the air was transported directly from British Columbia, where prior dust measurements were conducted (Leaitch et al., 2009), to SPL. In comparison, the DOY 91–136 (peak spring season) average Ångström exponent for 2004 is 1.09 ± 0.005 , and the average AOD is 0.075 ± 0.069 . The spring average Ångström for 2006 is 0.56 ± 0.010 with an average AOD of 0.07 ± 0.001 . Although these two years have similar aerosol loading, as represented by the optical depths, the size of the aerosol and thus likely the composition is significantly different. As documented in the literature, severe Asian dust storms impacted Beijing and Korea, eventually reaching North America in April and May of 2006 (e.g. Papayannis et al., 2007; Lee et al., 2008; Leaitch et al., 2009). These average AOD and α_{MFRSR} values for the known Asian dust event are quite similar to many springtime daily average values in the long-term MFRSR climatology at SPL, as shown in Fig. 4a. While not an absolute indication, they suggest that Asian dust is an important factor in the spring aerosol coarse-mode composition and total AOD at SPL. Significant Asian dust storms were not observed during the timeframe when nephelometer data are available.

The regional dust events plotted on Figs. 4 (large green symbols) are consistent with typical springtime measurements (small green dots) of the Ångström exponent

Contributions of dust and biomass-burning to aerosols at a Colorado mountain-top site

A. G. Hallar et al.

[Title Page](#)[Abstract](#)[Introduction](#)[Conclusions](#)[References](#)[Tables](#)[Figures](#)[◀](#)[▶](#)[◀](#)[▶](#)[Back](#)[Close](#)[Full Screen / Esc](#)[Printer-friendly Version](#)[Interactive Discussion](#)

and events, so we are relying on the climatological values obtained from these instruments to represent typical conditions of the column and at the surface (3220 m a.s.l.). The strong springtime increase in AOD in the MFRSR is not observed in the in situ nephelometer light scattering data. Additionally, the springtime decrease in Ångström exponent is more pronounced in the MFRSR data, compared to the in situ surface data. Thus, dust events are less distinguishable in the in situ data than the column measurement, suggesting that a significant amount of dust may be found above the elevation of SPL. This conclusion is further supported by the relatively invariant AOD signal across the day, suggesting that the majority of the aerosol population observed by the MFRSR at SPL is not influenced by the boundary layer via mountain wave dynamics (i.e. diurnal upslope and downslope flow).

These results are supported by previous in situ, modeling and remote sensing studies suggesting a more pronounced dust layer at higher elevations. Initially, with three sites in California located at different elevations (Trinidad Head, Trinity Alps, and Mount Lassen), VanCuren et al. (2005) demonstrated a distinct separation in aerosol chemistry between the stable marine boundary layer and the troposphere during the spring of 2002. Using eight-stage rotating drum impactors analyzed in 3 h time steps by x-ray fluorescence, VanCuren et al. (2005) categorized Asian dust by using a Fe/Ca ratio. Continuous Asian aerosol transport was found above the boundary layer, and Mount Lassen (1755 m a.s.l.) was dominated by Asian continental aerosols, especially under conditions of strong synoptic forcing in the spring. Creamean et al. (2014) expanded upon VanCuren et al. (2005), using 10 years of IMPROVE data from 25 sites along the United States West Coast, including 15 mountain sites. They found the highest concentration of Asian dust at the high elevations, due to the increased exposure to the free troposphere in comparison to the coastal sites, and peak concentrations in the spring at all sites. Wells et al. (2007) also saw a spring increase in dust concentration at high elevations attributed to intercontinental transport. Specifically, IMPROVE measurements and simulations from the Navy Aerosol Analysis and Prediction System of PM₁₀ soil showed a two-fold increase at a high altitude site (Sawtooth National Forest,

Contributions of dust and biomass-burning to aerosols at a Colorado mountain-top site

A. G. Hallar et al.

[Title Page](#)[Abstract](#)[Introduction](#)[Conclusions](#)[References](#)[Tables](#)[Figures](#)[◀](#)[▶](#)[◀](#)[▶](#)[Back](#)[Close](#)[Full Screen / Esc](#)[Printer-friendly Version](#)[Interactive Discussion](#)

Idaho, 1980 m.a.s.l.) compared to a low altitude site (Kalmiopiss, Oregon, 90 m.a.s.l.) in the spring from 2001–2004. In May 2007, measurements from the Cloud–Aerosol Lidar with Orthogonal Polarization (CALIOP) observed dust clouds generated during a storm in China’s Taklimakan Desert lofted to the upper troposphere (8–10 km) and transported more than one full circuit around the globe (Uno et al., 2009). Similar to the dynamic processes described by VanCuren et al. (2005), subsidence of a large-scale high-pressure system caused the dust layer to descend into the lower troposphere (Uno et al., 2009). Yu et al. (2010) reported that CALIOP also observed dust layers between 4–6 km across the northwestern Pacific (from 0–50° N and from 50–140° E) during the spring of 2007; this study was followed by work by Huang et al. (2014) demonstrating similar results for each April from 2007–2012. Again these prior studies are consistent with the conclusion that a significant amount of dust may be found above the elevation of SPL in the spring.

While dust (local and/or Asian) has a large seasonal impact on aerosol loading at SPL, our results also indicate that smoke may have a similar impact based on similar median AOD values for a dust-dominated spring (0.06) and a smoke-dominated summer (0.07). The SPL dataset highlights the potential wide scale implications of a warmer drier climate on aerosol loading in the western United States increased drought in the western United States will result in increased wildfire activity and dust events. Dennison et al. (2014) demonstrated increasing trends in the number of large fires, most significant for mountain ecosystems, coinciding with increasing drought severity. The impact of drought is clearly evident within this data set. For example, in 2002, record or near-record precipitation deficits were observed throughout the western United States (Cook et al., 2004), creating conditions conducive to the very large Hayman fire (Schoennagel et al., 2004) in Colorado. The Hayman fire had a significant impact on the AOD at SPL, nearly 250 km north of the fire, resulting in the anomalously high summer AOD shown Fig. 2, along with the direct impact of the fire denoted in Fig. 4.

Contributions of dust and biomass-burning to aerosols at a Colorado mountain-top site

A. G. Hallar et al.

Title Page

Abstract

Introduction

Conclusions

References

Tables

Figures

◀

▶

◀

▶

Back

Close

Full Screen / Esc

Printer-friendly Version

Interactive Discussion

Depending upon its severity, increased aerosol loading in the western United States has many implications including effects on visibility, air quality and climate feedbacks. Collaud Coen et al. (2013) studied long-term (> 10 years) trends in aerosol scattering from 24 observatories across the globe. The Mount Zirkel Wilderness IMPROVE site, a few kilometers away from SPL, was an anomaly compared to most of the stations studied, because it showed an increasing trend for aerosol scattering coefficient (+4 % decade⁻¹). Mount Zirkel represents the only high altitude IMPROVE site (> 2.5 km) in the United States Intermountain West with a long-term aerosol scattering record. Also using IMPROVE network data from 1990–2004, Murphy et al. (2011) found that in contrast to other seasons, elemental carbon (EC) increased in the summer within the Intermountain West, due to an increase in summer wildfires. Hand et al. (2011) found an increase in fine soil concentrations in the Intermountain West from 1989–2008 via the IMPROVE dataset, and this increase was most prominent in the springtime. The Intermountain West will continue to face significant difficulties maintaining mandated visibility faced with a drier climate, as there is a broad consensus among climate models that the Intermountain West will become more arid in the 21st century (e.g., Seager et al., 2007). Changes in aerosol loading, from increased wildfires and dust events, will have a direct impact on visibility, climate, and air quality (Val Martin et al., 2015). The results presented here suggest that biomass burning in the summer and spring time dust have had a significant impact in the Intermountain West over the last decade, however, emissions of these “natural” aerosols cannot be controlled in the same way that emissions from anthropogenic sources can be.

7 Conclusions

In the remote western United States, the role of seasonal dust and smoke in the aerosol population is an important issue for climate predictions and preserving visibility in pristine locations. Using the long-term vis-MFRSR and in situ aerosol optical data, the composition of spring and summer aerosol at SPL was investigated. The data clearly

**Contributions of dust
and biomass-burning
to aerosols at
a Colorado
mountain-top site**

A. G. Hallar et al.

Title Page

Abstract

Introduction

Conclusions

References

Tables

Figures

◀

▶

◀

▶

Back

Close

Full Screen / Esc

Printer-friendly Version

Interactive Discussion

ties over the western North Atlantic Ocean at Bermuda, *Atmos. Chem. Phys.*, 14, 7617–7629, doi:10.5194/acp-14-7617-2014, 2014.

Asmi, A., Collaud Coen, M., Ogren, J. A., Andrews, E., Sheridan, P., Jefferson, A., Weingartner, E., Baltensperger, U., Bukowiecki, N., Lihavainen, H., Kivekäs, N., Asmi, E., Aalto, P. P., Kulmala, M., Wiedensohler, A., Birmili, W., Hamed, A., O'Dowd, C., G Jennings, S., Weller, R., Flentje, H., Fjaeraa, A. M., Fiebig, M., Myhre, C. L., Hallar, A. G., Swietlicki, E., Kristensson, A., and Laj, P.: Aerosol decadal trends – Part 2: In-situ aerosol particle number concentrations at GAW and ACTRIS stations, *Atmos. Chem. Phys.*, 13, 895–916, doi:10.5194/acp-13-895-2013, 2013.

Augustine, J. A., Hodges, G. B., Dutton, E. G., Michalsky, J. J., and Cornwall, C. R.: An aerosol optical depth climatology for NOAA's national surface radiation budget network (SURFRAD), *J. Geophys. Res.*, 113, D11204, doi:10.1029/2007JD009504, 2008.

Belnap, J. and Gillette, D. A.: Vulnerability of desert biological soil crusts to wind erosion: the influences of crust development, soil texture, and disturbance, *J. Arid Environ.*, 39, 133–142, 1998.

Bigelow, D. S., Slusser, J. R., Beaubien, A. F., and Gibson, J. H.: The USDA ultraviolet radiation monitoring program, *B. Am. Meteorol. Soc.*, 79, 601–615, 1998.

Bodhaine, B. A.: Aerosol measurements during the Mauna Loa Photochemistry Experiment 2, *J. Geophys. Res.*, 101, 14757–14766, 1996.

Borys, R. D. and Wetzel, M. A.: Storm Peak Laboratory: a research, teaching and service facility for the atmospheric sciences, *B. Am. Meteorol. Soc.*, 78, 2115–2123, 1997.

Boucher, O., Randall, D., Artaxo, P., Bretherton, C., Feingold, G., Forster, P., Kerminen, V.-M., Kondo, Y., Liao, H., Lohmann, U., Rasch, P., Satheesh, S. K., Sherwood, S., Stevens, B., and Zhang, X. Y.: Clouds and aerosols, in: *Climate Change 2013: The Physical Science Basis. Contribution of Working Group I to the Fifth Assessment Report of the Intergovernmental Panel on Climate Change*, edited by: Stocker, T. F., Qin, D., Plattner, G.-K., Tignor, M., Allen, S. K., Boschung, J., Nauels, A., Xia, Y., Bex, V., and Midgley, P. M., Cambridge University Press, Cambridge, UK and New York, NY, USA, 2013.

Clarke, A. and Kapustin, V.: Hemispheric aerosol vertical profiles: anthropogenic impacts on optical depth and cloud nuclei, *Science*, 329, 1488–1492, 2010.

Clarke, A., McNaughton, C., Kapustin, V., Shinozuka, Y., Howell, S., Dibb, J., Zhou, J., Anderson, B., Brekhovskikh, V., Turner, H., and Pinkerton, M.: Biomass burning and pollution aerosol over North America: organic components and their influence on spec-

port, ISSN:0737-5352-87, available at: <http://vista.cira.colostate.edu/improve/Publications/Reports/2011/2011.htm> (last access: 5 August 2015), 2011.

Hand, J. L., Schichtel, B. A., Malm, W. C., Copeland, S., Molenaar, J. V., Frank, N., and Pitchford, M.: Widespread reductions in haze across the United States from the early 1990s through 2011, *Atmos. Environ.*, **94**, 671–679, 2014.

Harrison, L. and Michalsky, J.: Objective algorithms for the retrieval of optical depths from ground-based measurement, *Appl. Optics*, **33**, 5126–5132, 1994.

Heald, C. L., Jacob, D. J., Park, R. J., Alexander, B., Fairlie, T. D., Yantosca, R. M., and Chu, D. A.: Transpacific transport of Asian anthropogenic aerosols and its impact on surface air quality in the United States, *J. Geophys. Res.-Atmos.*, **111**, D14310, doi:10.1029/2005JD006847, 2006.

Hoerling, M., Eischeid, J., Kumar, A., Leung, R., Mariotti, A., Mo, K., Schubert, S., and Seager, R.: Causes and predictability of the 2012 Great Plains Drought, *B. Am. Meteorol. Soc.*, **95**, 269–282, doi:10.1175/BAMS-D-13-00055.1, 2014.

Jaffe, D. A., Snow, J., and Cooper, O.: The 2001 Asian Dust Event: transport and impact on surface aerosol concentrations in the United States, *EOS T. Am Geophys. Un.*, **84**, 501–507, doi:10.1029/2003EO460001, 2003.

Kavouras, I. G., Etyemezian, V., Dubois, D. W., and Xu, J.: Source reconciliation of atmospheric dust causing visibility impairment in Class I areas of the western United States, *J. Geophys. Res.*, **114**, D02308, doi:10.1029/2008JD009923, 2009.

Kennedy, M. C. and Johnson, M. C.: Fuel treatment prescriptions alter spatial patterns of fire severity around the wildland–urban interface during the Wallow Fire, Arizona, USA, *Forest Ecol. Manag.*, **318**, 122–132, 2014.

Landry, C. C., Buck, K. A., Raleigh, M. S., and Clark, M. P.: Mountain system monitoring at Senator Beck Basin, San Juan Mountains, Colorado: a new integrative data source to develop and evaluate models of snow and hydrologic processes, *Water Resour. Res.*, **50**, 1773–1788, doi:10.1002/2013WR013711, 2014.

Leaitch, W. R., Macdonald, A. M., Anlauf, K. G., Liu, P. S. K., Toom-Sauntry, D., Li, S.-M., Liggio, J., Hayden, K., Wasey, M. A., Russell, L. M., Takahama, S., Liu, S., van Donkelaar, A., Duck, T., Martin, R. V., Zhang, Q., Sun, Y., McKendry, I., Shantz, N. C., and Cubison, M.: Evidence for Asian dust effects from aerosol plume measurements during INTEX-B 2006 near Whistler, BC, *Atmos. Chem. Phys.*, **9**, 3523–3546, doi:10.5194/acp-9-3523-2009, 2009.

Contributions of dust and biomass-burning to aerosols at a Colorado mountain-top site

A. G. Hallar et al.

Title Page

Abstract

Introduction

Conclusions

References

Tables

Figures

◀

▶

◀

▶

Back

Close

Full Screen / Esc

Printer-friendly Version

Interactive Discussion

Contributions of dust and biomass-burning to aerosols at a Colorado mountain-top site

A. G. Hallar et al.

Title Page

Abstract

Introduction

Conclusions

References

Tables

Figures

◀

▶

◀

▶

Back

Close

Full Screen / Esc

Printer-friendly Version

Interactive Discussion

- Lee, Y.-G. and Cho, C. H.: Characteristics of aerosol size distribution for a severe Asian dust event observed at Anmyeon, Korea in April 2006, *J. Korean Meteor. Soc.*, 43, 87–96, 2007.
- Lowenthal, D. H., Borys, R. D., and Wetzel, M. A.: Aerosol distributions and cloud interactions at a mountaintop laboratory, *J. Geophys. Res.*, 107, 4345, doi:10.1029/2001JD002046, 2002.
- 5 Michalsky, J. and LeBaron, B.: Fifteen-year aerosol optical depth climatology for Salt Lake City, *J. Geophys. Res.-Atmos.*, 118, 3271–3277, doi:10.1002/jgrd.50329, 2013.
- Michalsky, J. J., Schlemmer, J. A., Berkheiser, W. E., Berndt, J. L., Harrison, L. C., Laulainen, N. S., Larson, N. R., and Barnard, J. C.: Multiyear measurements of aerosol optical depth in the Atmospheric Radiation Measurement and Quantitative Links programs, *J. Geophys. Res.-Atmos.*, 106, 12099–12107, 2001.
- 10 Murphy, D. M., Chow, J. C., Leibensperger, E. M., Malm, W. C., Pitchford, M., Schichtel, B. A., Watson, J. G., and White, W. H.: Decreases in elemental carbon and fine particle mass in the United States, *Atmos. Chem. Phys.*, 11, 4679–4686, doi:10.5194/acp-11-4679-2011, 2011.
- Neff, J. C., Ballantyne, A. P., Farmer, G. L., Mahowald, N. M., Conroy, J., Landry, C. C., Overpeck, J., Painter, T. H., Lawrence, C. R., and Reynold, R.: Recent increases in eolian dust deposition due to human activity in the western United States, *Nat. Geosci.*, 1, 189–195, doi:10.1038/ngeo133, 2008.
- 15 Obrist, D., Hallar, A. G., McCubbin, I., Stephens, B. B., and Rahn, T.: Atmospheric mercury concentrations at Storm Peak Laboratory in the Rocky Mountains: Evidence for long-range transport from Asia, boundary layer contributions, and plant mercury uptake, *Atmos. Environ.*, 42, 7579–7589, 2008.
- Painter, T. H., Barrett, A. P., Landry, C. C., Neff, J. C., Cassidy, M. P., Lawrence, C. R., McBride, K. E., and Farmer, G. L.: Impact of disturbed desert soils on duration of mountain snow cover, *Geophys. Res. Lett.*, 34, L12502, doi:10.1029/2007GL030284, 2007.
- 25 Painter, T. H., Deems, J. S., Belnap, J., Hamlet, A. F., Landry, C. C., and Udall, B.: Response of Colorado River runoff to dust radiative forcing in snow, *P. Natl. Acad. Sci. USA*, 107, 17,125–17,130, doi:10.1073/pnas.0913139107, 2010.
- Painter, T. H., Bryant, A. C., and Skiles, S. M.: Radiative forcing by light absorbing impurities in snow from MODIS surface reflectance data, *Geophys. Res. Lett.*, 39, L17502, doi:10.1029/2012GL052457, 2012.
- 30 Papayannis, A., Zhang, H. Q., Amiridis, V., Ju, H. B., Chourdakis, G., Georgoussis, G., Pérez, C., Chen, H. B., Goloub, P., Mamouri, R. E., Kazadzis, S., Paronis, D., Tsaknakis, G., and Baldasano, J. M.: Extraordinary dust event over Beijing, China, during April 2006: Lidar, Sun

- Westerling, A. L., Hidalgo, H. G., Cayan, D. R., and Swetnam, T. W.: Warming and earlier spring increase western United States forest wildfire activity, *Science*, 313, 940–943, 2006.
- Uno, I., Eguchi, K., Yumimoto, K., Takemura, T., Shimizu, A., Uematsu, M., Liu, Z., Wang, Z., Hara, Y., and Sugimoto, N.: Asian dust transported one full circuit around the globe, *Nat. Geosci.*, 2, 557–560, 2009.
- 5 Yu, H., Remer, L. A., Chin, M., Bian, H., Kleidman, R. G., and Diehl, T.: A satellite-based assessment of transpacific transport of pollution aerosol, *J. Geophys. Res.-Atmos.*, 113, D14S12, doi:10.1029/2007JD009349, 2008.
- 10 Yu, H., Remer, L. A., Chin, M., Bian, H., Tan, Q., Yuan, T., and Zhang, Y.: Aerosols from overseas rival domestic emissions over North America, *Science*, 337, 566–569, 2012.

Contributions of dust and biomass-burning to aerosols at a Colorado mountain-top site

A. G. Hallar et al.

[Title Page](#)[Abstract](#)[Introduction](#)[Conclusions](#)[References](#)[Tables](#)[Figures](#)[Back](#)[Close](#)[Full Screen / Esc](#)[Printer-friendly Version](#)[Interactive Discussion](#)

Table 1. Dust and biomass burning events observed at SPL.

Start time (UTC)	End time (UTC)		MFRSR data available	Nephelometer data available
DUST EVENT				
15 Apr 2001 12:00	16 Apr 2001 12:00	Asian	X	
27 Apr 2006	1 May 2006	Asian	X	
<i>Regional Events</i>		Wind Dir. at CSAS		
19 Apr 2007 19:00	20 Apr 2007 07:00	201	X	
16 Apr 2008 19:00	17 Apr 2008 07:00	219	X	
4 Apr 2009 05:00	5 Apr 2009 07:00	206	X	
13 Apr 2010 08:00	13 Apr 2010 13:00	188	X	
22 May 2010 09:00	24 May 2010 15:00	192	X	
22 Apr 2011 22:00	24 Apr 2011 00:00	258		X
1 May 2011 12:00	4 May 2011 06:00	279		X
5 May 2011 09:00	11 May 2011 06:00	206	X	X
27 May 2011 18:00	29 May 2011 12:00	243		X
7 Mar 2012 09:00	8 Mar 2012 09:00	197		X
20 Mar 2012 09:00	22 Mar 2012 00:00	193		X
27 Mar 2012 18:00	29 Mar 2012 12:00	207		X
2 Apr 2012 20:00	3 Apr 2012 10:00	198		X
7 Apr 2012 18:00	11 Apr 2012 14:00	201		X
20 May 2012 00:00	23 May 2012 14:00	213		X
24 May 2012 14:00	1 Jun 2012 00:00	217*		X
25 May 2013 00:00	25 May 2013 18:00	207		X
FIRE EVENT				
27 Jul 2000	6 Aug 2000	Origin		
15 Jun 2002	10 Jul 2002	NW US 1	X	
30 Jul 2002	3 Aug 2002	Hayman	X	
4 Sep 2006	9 Sep 2006	AR, OR, CA	X	
29 Aug 2009	3 Sep 2009	CA	X	
4 Jun 2011 07:00	8 Jun 2011 00:00	Station Fire	X	
30 Jun 2012 07:00	5 Jul 2012 07:00	Wallow	X	X
10 Aug 2012 07:00	18 Aug 2012 07:00	Waldo/High Park		X
21 Sep 2012 07:00	23 Sep 2012 07:00	NW US 2		X
		NW US 3	X	X

* Average of 3 consecutive dust events at CSAS.

Contributions of dust and biomass-burning to aerosols at a Colorado mountain-top site

A. G. Hallar et al.

Title Page

Abstract Introduction

Conclusions References

Tables Figures

◀ ▶

◀ ▶

Back Close

Full Screen / Esc

Printer-friendly Version

Interactive Discussion



Contributions of dust and biomass-burning to aerosols at a Colorado mountain-top site

A. G. Hallar et al.

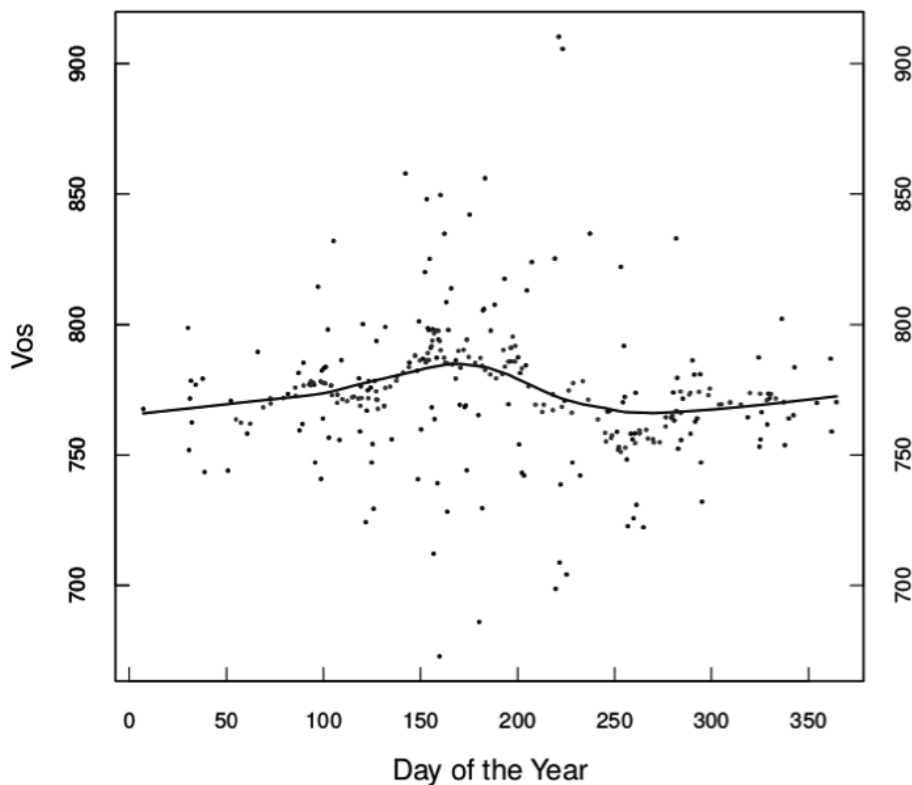


Figure 1. Calibration results for the 415 nm channel from vis-MFRSR Langley plots. All V_o 's from the Langleys are shown with dots. The lowest estimate (black curve) is used for the assigned V_o 's in the aerosol optical depth analyses.

[Title Page](#)[Abstract](#)[Introduction](#)[Conclusions](#)[References](#)[Tables](#)[Figures](#)[◀](#)[▶](#)[◀](#)[▶](#)[Back](#)[Close](#)[Full Screen / Esc](#)[Printer-friendly Version](#)[Interactive Discussion](#)

Contributions of dust and biomass-burning to aerosols at a Colorado mountain-top site

A. G. Hallar et al.

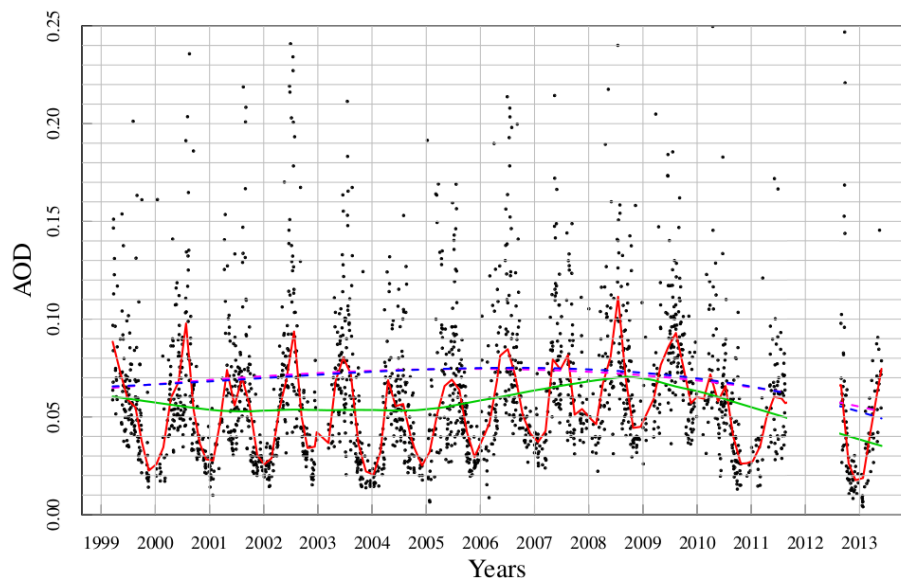


Figure 2. Black dots are 2252 daily averages of AOD at 500 nm. The red line is a lowess fit with a three-month window. The green line is a lowess fit with a five-year window. The blue dashed line is a least squares fit to a cubic polynomial. A year-gap in the MFRSR measurements occurred in 2011–2012. This interruption in MFRSR operation was due to structural renovations at the SPL facility.

[Title Page](#)[Abstract](#)[Introduction](#)[Conclusions](#)[References](#)[Tables](#)[Figures](#)[◀](#)[▶](#)[◀](#)[▶](#)[Back](#)[Close](#)[Full Screen / Esc](#)[Printer-friendly Version](#)[Interactive Discussion](#)

Contributions of dust and biomass-burning to aerosols at a Colorado mountain-top site

A. G. Hallar et al.

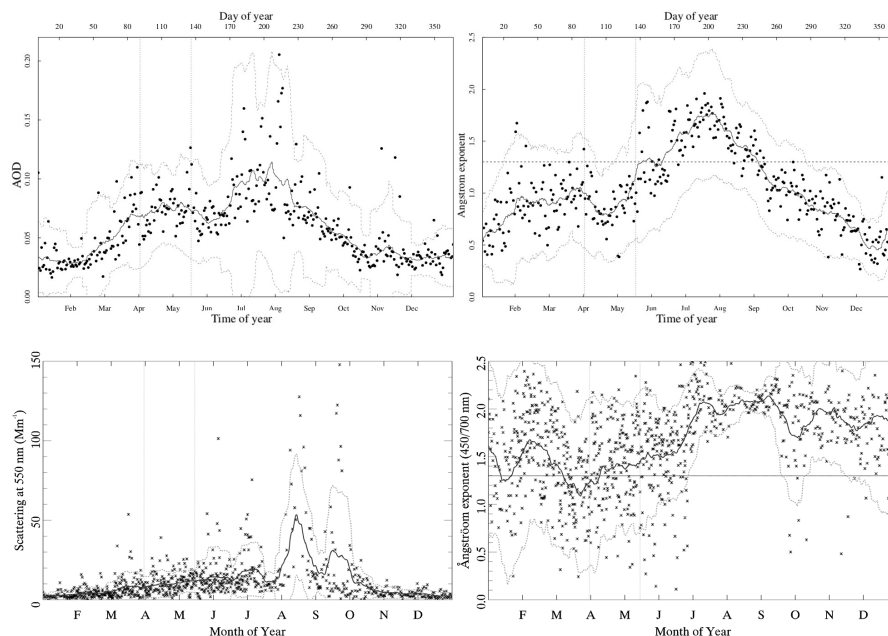
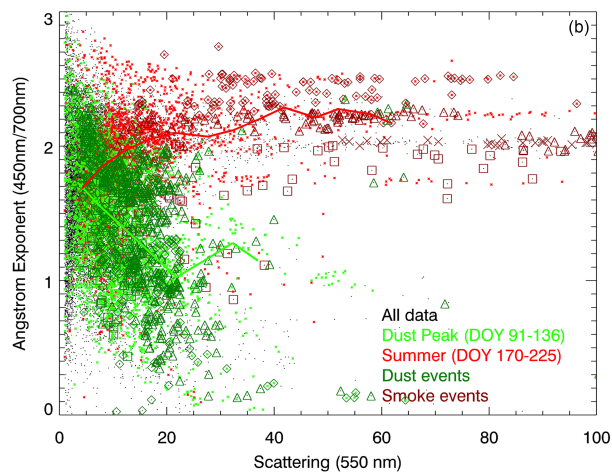
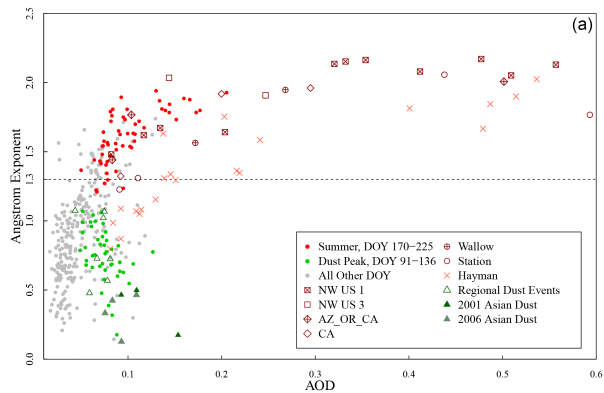


Figure 3. Left top panel shows seasonal pattern in AOD at 500 nm using data from 1999–2011 and 2013. Right top panel presents seasonal pattern in Ångström exponent (500 nm/870 nm) for the same time range. Bottom panel shows seasonal pattern in nephelometer scattering and Ångström exponent. In all plots, the black dots are daily averages of the data. The dark grey line is a running average, calculated hourly using the data spanning ten days before and after each position. The light grey lines indicate the standard deviation vertically from the running average. Vertical grey dashed lines denote the peak dust period, approximately 1 April–15 May (DOY 91–136). The Ångström exponent of 1.3 is highlighted with a dashed vertical line for instruments.

Contributions of dust and biomass-burning to aerosols at a Colorado mountain-top site

A. G. Hallar et al.



Title Page

Abstract

Introduction

Conclusions

References

Tables

Figures



Back

Close

Full Screen / Esc

Printer-friendly Version

Interactive Discussion



Figure 4. (a) AOD vs. Ångström measurements for vis-MFRSR. The dots represent daily-averaged measurements for the entire 1999–2011 and 2013 period of observation. The red indicates all measurements made from DOY 170–225 during peak summer season. Green indicates all measurements made during DOY 91–136, spring dust peak. The gray points indicate all measurements that were not made during these spring and summer periods. Events listed in Table 1 are shown with larger symbols; dust events are dark green, fire events are maroon. **(b)** Relationship between hourly averaged Ångström exponent and scattering from the 2011–2013 nephelometer measurements. The lines represent the median value of Ångström and scattering for each scattering bin for either the Dust Peak or Summer time range. The scattering bin limits are: [1, 5, 10, 15, 20, . . . , 95, 100] and at least 15 valid data points are required in each scattering bin to generate a line segment. Regional dust events from Table 1 are shown in dark green; smoke events from Table 1 are shown in maroon. For the dust events, diamonds represent data from 2011, triangles for 2012 and squares for 2013. For the smoke events, the Wallow fire is indicated by squares, the Front Range fire is indicated by diamonds, the NW1 fire is indicated by triangles and the NW2 fire is indicated by x symbols.

Contributions of dust and biomass-burning to aerosols at a Colorado mountain-top site

A. G. Hallar et al.

Title Page

Abstract

Introduction

Conclusions

References

Tables

Figures

◀

▶

◀

▶

Back

Close

Full Screen / Esc

Printer-friendly Version

Interactive Discussion